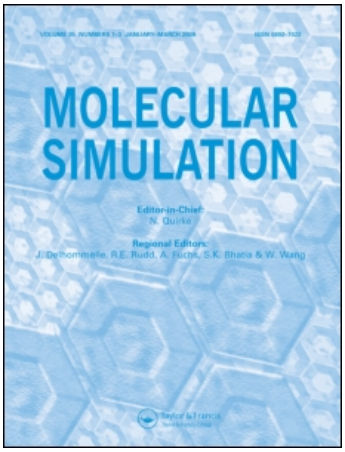

Molecular Simulation

Publication details, including instructions for authors and subscription information:
http://www.informaworld.com/smpp/title~content=t713644482

Investigating lithium ion conductivity in amorphous solids containing $[V_{10}O_{28}]^{6-}$ clusters by computer simulation

Lin-yin Wu[a]; Jun-min Liao[a]; Cheng-lung Chen[a]
[a] Department of Chemistry, National Sun Yat-sen University, Kaohsiung, ROC, Taiwan

To cite this Article Wu, Lin-yin , Liao, Jun-min and Chen, Cheng-lung(2007) 'Investigating lithium ion conductivity in amorphous solids containing $[V_{10}O_{28}]^{6-}$ clusters by computer simulation', Molecular Simulation, 33: 3, 269 — 276
To link to this Article: DOI: 10.1080/08927020601089056
URL: http://dx.doi.org/10.1080/08927020601089056

Molecular Simulation, Vol. 33, No. 3, 15 March 2007, 269–276

Taylor & Francis
Taylor & Francis Group

Investigating lithium ion conductivity in amorphous solids containing $[V_{10}O_{28}]^{6-}$ clusters by computer simulation

LIN-YIN WU, JUN-MIN LIAO and CHENG-LUNG CHEN*

Department of Chemistry, National Sun Yat-sen University, Kaohsiung, ROC 80424, Taiwan

(Received June 2006; in final form October 2006)

Computer simulation method was applied to investigate the migration of lithium ion in three amorphous solid systems containing polyoxovanadate (POV) clusters $[V_{10}O_{28}]^{6-}$. The cluster was adopted from a recently synthesized crystalline poly[octa-μ-aqua-octaaqua-μ-decavanadato-hexalithium] (POAODH). The simulated POV systems correspond to amorphous solid half-dehydrated solid and completely dehydrated solid doped with LiCl salt. The simulation results show large diffusion constants of lithium ions in all systems in spite of highly negatively charged $[V_{10}O_{28}]^{6-}$ clusters presented in the system. The estimated ionic conductivity due to the migration of lithium ions reaches a magnitude of 10^{-4} S/m. The conductivity increases as the water content in the system decreases. The analysis of moving trajectories shows the lithium ion moves around the oxygen sites of POV clusters and hops between them. The estimated displacement of lithium ion is about $4 \sim 5$ Å, which is much larger than the corresponding displacement of lithium ion in a polymer matrix. Rapidly rotating clusters shown by orientation correlation function analysis, in conjunction with the large separation between clusters in the system, provides favorable conditions for the large amplitude migration of lithium ions.

Keywords: MD; $[V_{10}O_{28}]^{6-}$ POV cluster; Lithium ion; Conductivity; Hopping

1. Introduction

Plastic crystalline substances can exhibit ionic conductivities. In some ionic plastic crystals containing lithium ion, the conductivities due to the motion of lithium ion can be as high as $4 \times 10^{-4}\,S\,m^{-1}$ [1–6]. The high conductivity is usually attributed due to the rotational disorder and lattice defects. The reorientational motion of sulfate-ion in ionic crystals, Li_2SO_4 and $LiAgSO_4$ had been detected by Raman spectroscopic method [7–9]. A class of plastic crystal ionic compounds involving alkylmethylpyrrolidinium cation and bis(trifluoromethanesulphonyl)imide anion (referred as P_{1x}) had conductivity between 10^{-5} and $10^{-7}\,S\,m^{-1}$ at ambient temperature below their melting points [10,11]. MacFarlane *et al.* has reported their experimental result of doping lithium ions into P_{1x} plastic crystalline matrix [12]. The measured fast ion conductivity is $2 \times 10^{-2}\,S\,m^{-1}$ at 60°C. This is due to the solid–solid phase transition and hence increases the disorder of the solid substance. This new class of ionic crystalline materials may replace the traditional polymer–lithium salt materials for high energy rechargeable batteries. Most of solid polymer electrolytes are poor ionic conductors and have room temperature conductivities of about $10^{-2}\,S\,m^{-1}$ or less [13–17]. Practical applications require conductivities in the range of 10^{-2}–$10^{-1}\,S\,m^{-1}$. The motion of ions in polymer matrix is mediated by the dynamics of host polymer, thereby restricting the conductivity to relatively low values. Some theoretical calculations have been carried out for understanding the ionic conduction mechanism in the matrices of polymer electrolytes [18–28]. Duan *et al.* has reported their molecular dynamics (MD) simulation of lithium–polyethylene oxide (PEO) system at room temperature and obtained diffusive constant of lithium ion close to an experimentally measured value [29]. The work indicated that the most significant motion leading to large diffusion constant is due to the Li^+ hopping between oxygen atoms on PEO units.

Recently, Ma *et al.* has synthesized a special polyoxovanadate (POV) crystal [30], poly[octa-μ-aqua-octaaqua-μ-decavanadato-hexalithium] (POAODH). The unit cell of POAODH has fairly large dimensions, $(a,b,c) = (17.6,\ 10.3$ and 9.2 Å), and contains a large $[V_{10}V_{28}]^{6-}$ cluster linked by centrosymmetric $[Li_6(H_2O)_{16}]^{6+}$ chains. The structure of this crystal

*Corresponding author. Email: chen1@mail.nsysu.edu.tw

Molecular Simulation
ISSN 0892-7022 print/ISSN 1029-0435 online © 2007 Taylor & Francis
http://www.tandf.co.uk/journals
DOI: 10.1080/08927020601089056

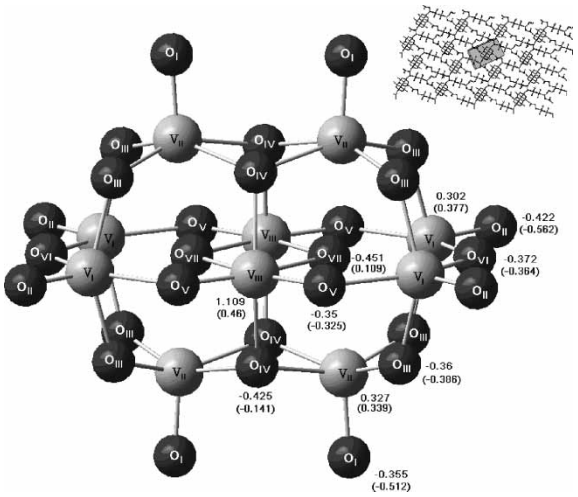

Figure 1. The structure and atomic charges of $[V_{10}O_{28}]^{6-}$ cluster. Atomic charges without parenthesis are obtained by DFT method and those in parenthesis are obtained by ZINDO calculation.

is shown in the top right corner of figure 1. The crystal can be regarded as a salt-like mixture containing highly negatively charged $[V_{10}V_{28}]^{6-}$ clusters, positive charged lithium ions and water. The quantum mechanical calculation with density functional theory (DFT) method of $[V_{10}O_{28}]^{6-}$ showed very small differences in bond lengths and angles of the optimized geometry from its crystalline structure [31–33]. This result indicates that $[V_{10}O_{28}]^{6-}$ cluster is very stable in spite of its high negative charges. The negative charges are distributed over oxygen atoms in the cluster and forms many coordination sites available for lithium ions. In figure 1 we show the structure of the $[V_{10}O_{26}]^{6-}$ cluster adopted from the reported crystalline structure. Two sets of atomic charges obtained by DFT and a semiempirical quantum mechanical method, ZINDO [34], are also shown in the figure. The oxygen atoms and vanadium atoms in the cluster can be grouped into seven (O_I–O_{VII}) and three (V_I–V_{III}) different types according to their symmetries. The (O_I–O_{VI}) oxygen atoms are on the outer region of the cluster and easy to form coordination with positive ions. These oxygen atoms are denoted as OC atoms. The O_{VII} oxygen atoms are wrapped in the interior of the cluster and are less probable to form coordination with other positive ions outside the cluster. These oxygen atoms are denoted as OF atoms. The symmetry group of the cluster is D_{2h} with its molecular z-axis along the O_{VI}–O_{VII}–O_{VII}–O_{VI} line. In the crystal, lithium ions and water molecules form chain like structure to link $[V_{10}O_{28}]^{6-}$ clusters, and result in a large spacing between them. Thermogravimetric analysis (TGA) results show that the weight loss of the crystal is around 22% in the range 343–583 K. This is compatible with the content of water (22.4 wt%) resulting from the theoretical value in the molecular formula [30]. According to this experiment, the water molecules can be removed from the crystal by simply heating the sample. Since the $[V_{10}O_{28}]^{6-}$ clusters are very stable, increasing the temperature of the system will destroy the linkage between lithium ions and waters to the $[V_{10}O_{28}]^{6-}$ cluster, and form amorphous solids. Under this condition, lithium ions and waters should become mobile in the system due to the large spacing and various interaction forces. The mobility of the lithium ions is directly related to the conductivity of the material. The main goal of the current work is to investigate the ionic conductivity of this particular material by simulation method.

2. Simulation

Full atom MD simulations were carried out to investigate the migration of lithium ions in three systems containing POV clusters. System I is an amorphous POAODH solid. System II is a half-dehydrated amorphous POAODH solid, in which half amount of water molecules are removed from system I. System III is a completely dehydrated amorphous POAODH solid further doped with LiCl salt. The initial structure of system I was constructed by grouping $2 \times 3 \times 3$ unit cells of POAODH. The structure of unit cell was adopted directly from the reported crystalline structure [30]. The system contains 36 $[V_{10}O_{28}]^{6-}$ clusters, 576 water molecules and 216 lithium ions. Dimensions and density of the system are $(a,b,c) = (35.232,\ 30.957,\ 27.705\,\text{Å}$ and $2.549\,\text{g/cm}^3$. The annealed-quench dynamics MD runs were carried out from 300 to 600 K of this system with fixed dimensions of the cell. After the annealed-quench process, the crystalline structure of POAODH was destroyed. Energy minimization process with fixed cell dimension was carried out. This minimized system was used to initiate a consecutive MD run. Conventional MD run was carried out and the simulation temperature was set to 300 K. To construct initial positions of the half-hydrated POAODH System II, half amount of water molecules were removed from system I. Similar process with an annealed-quenched MD run followed by energy-minimization was carried out. During the energy minimization process, the dimensions of the cell were allowed to vary but the angles ($\alpha,\beta,r = 90°$) were fixed. The minimized dimensions of the cell and density were $(a,\ b,\ c) = (38.82,\ 30.568,\ 25.892\,\text{Å}$ and $2.227\,\text{g/cm}^3$. This energy minimized cell was used to initiate a consecutive MD run. To construct completely dehydrated POAODH system III, all water molecules were removed from system II and extra LiCl salt of 128 Li^+ and Cl^- ions were added into the system. The Li^+ and Cl^- ions were placed randomly in the system and similar procedure as the construction of system II was carried out. The final dimension of the energy minimized cell were $(a,\ b,\ c) = (34.844,\ 37.352,\ 26.833\,\text{Å}$ and the density of the system was $2.295\,\text{g/cm}^3$. This system was then subjected to MD runs as others. In all simulations atomic partial charges of POV were adopted from ZINDO calculations. Those charges obtained by DFT method are usually not appropriate to evaluate columbic interactions classically. The charges of lithium and chloride ions were assigned to $+1$ and -1. The partial charges of atoms

on water molecule were assigned to 0.42 for H and −0.84 for O (denoted as OW) as the assignment of TIPS force field [35]. DREIDING force field [36] was selected to carry out the MD simulations because this force field includes force field parameters of all elements in the system and also takes into account of specific hydrogen bonding interactions. Since our systems contains many ions and partially charged atoms, therefore, Ewald summation method [37] which counts charge–charge interactions for repeated periodic cells was employed. All simulations were performed on a SGI workstation using molecular modeling package Cerius 2 [38].

3. Results and discussion

Given in figure 2 are side views of the original unit cell and a snapshot of system I after 20 ps MD runs. The figure shows that $[V_{10}O_{28}]^{6-}$ clusters are no longer in the ordered array after the MD run. A similar disordered array was also found for systems II and III. Therefore, these systems can be regarded as amorphous solids. Based on the Einstein–Stoke equation, the diffusion constant, D, of a particular ion can be evaluated from its mean square displacement (MSD),

$$D = \lim_{t\to\infty} \frac{1}{6t} \left\langle \left| \vec{R}(t) - \vec{R}(0) \right|^2 \right\rangle$$

In which, $\vec{R}$ is the position vector of ion and t is the time-lag, respectively. Given in table 1 are the calculated diffusion constants of various ions and atoms of the three simulated systems. The mobility of $[V_{10}O_{28}]^{6-}$ cluster can be related to the diffusion constants of atoms OF, OC and V in the cluster. The table shows that D_{OF}, D_{OC} and D_V increase rapidly from hydrated system I to completely dehydrated system III. This indicates that mobility of cluster increases as the amount of water molecules are reduced from the system. The motion of clusters destroys the crystalline structure of the system and leads to an non-ordered array. The diffusion constants of OF, OC and V are found much smaller than other ions and water in these systems. This means that ions and water are much mobile than clusters. The table shows that D_{Li^+} increases by decreasing the water content of the system. For completely dehydrated system III, the diffusion constant D_{Li^+} is about three times larger than hydrated system I. The calculated diffusion constants of Li^+ are in the order of $10^{-11}\,m^2/s$, which is an order larger than the typical value of Li^+ in PEO matrix [18–29]. The calculated D_{OW} has the same magnitude as D_{Li^+} table 1 shows that D_{Li^+} is larger than D_{OW} in system I but is smaller than D_{OW} in system II. This indicates that Li^+ does not move simultaneously along with oxygen on water. In system III, we found that D_{Cl^-} is much smaller than D_{Li^+}. This indicates that Li^+ and Cl^- do not form ionic clusters. Some theoretical studies of Li salt in PEO polymer systems indicate that lithium ion

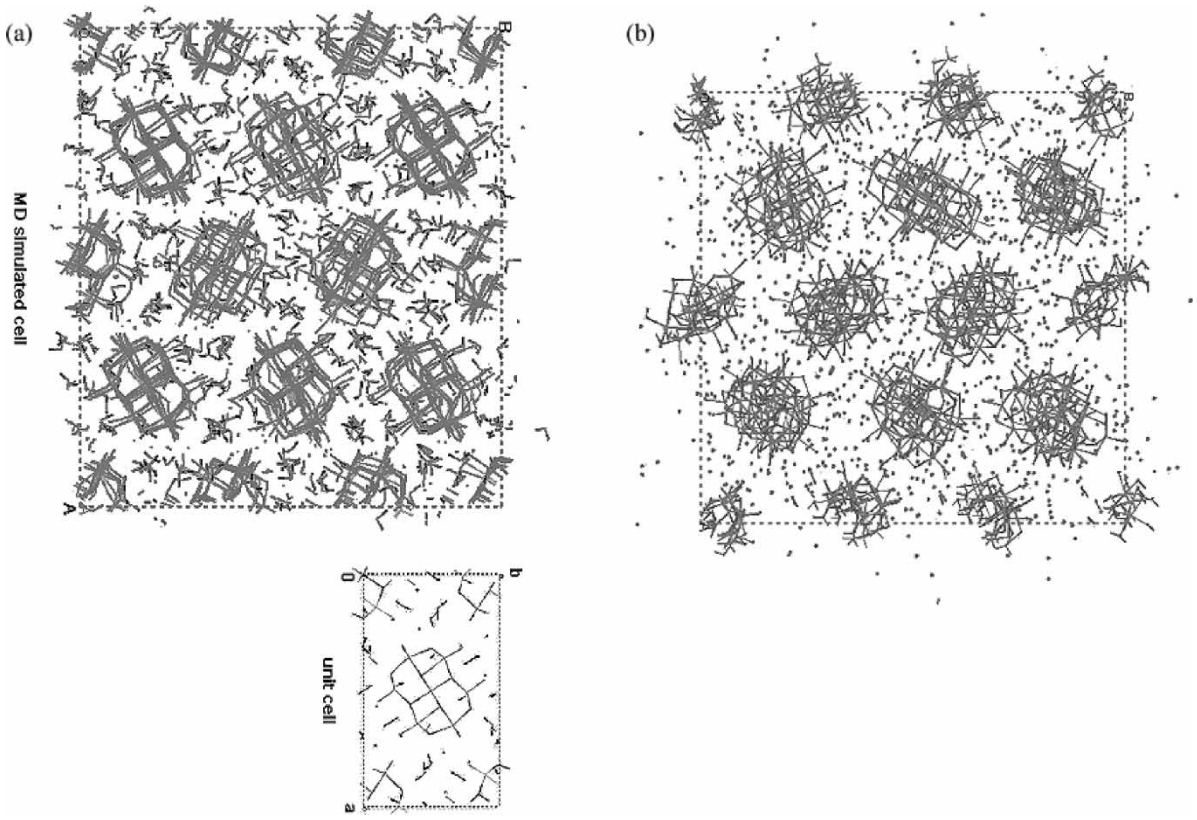

Figure 2. (a) Side views of unit cell and a snapshot of system I after 20 ps MD simulation; (b) side view of a snapshot of completely dehydrated system III after 20 ps MD simulation.

Table 1. Calculated diffusion constants (10^{-11} m^2/s) of various ions and atoms in three simulated systems.

System	Li^+	*OC*	*OW*	*OF*	*V*	Cl^-
I	2.15	0.57	1.37	0.22	0.30	
II	4.32	0.83	5.58	0.50	0.65	
III	7.08	2.22		2.12	1.72	4.02

tends to coordinate with the ether oxygen in the PEO polymer matrix and moves very slowly along with the segmental torsion of the polymer. Although $[V_{10}O_{28}]^{6-}$ cluster is more negatively charged than oxygen atoms in PEO, however, the results of diffusion constant calculations indicate that these highly charged clusters do not prevent the motion of Li^+. Our results indicate that neither does Li^+ stick on the $[V_{10}O_{28}]^{6-}$ cluster nor on water as in the polymer matrix. The conductivity, λ, due to the moving of lithium ion can be estimated from the diffusion constant based on Einstein–Nerst equation,

$$\lambda = \frac{Dz^2F^2}{RT}$$

Where z and F are ion charge and Faraday's constant, D is diffusion constant, R is gas constant and T is absolute temperature, respectively. The calculated ionic conductivities due to the migration of Li^+ are 0.957, 1.176 and 3.55 S m^{-1} for systems I, II and III, respectively. These calculated ionic conductivities increase as the water content decreases in the system and are much larger than those reported ionic conductivities for Li/polymer [18–29] and Li-doped plastic crystal systems ($\sim 10^{-2}$ S m^{-1}) [10–12].

In addition to diffusion constant, radial distribution functions (RDF), $g(r)$, of specific pairs of ion to ion or ion to atom can be calculated,

$$g(r) = \frac{1}{\rho}\frac{dn}{4\pi r^2 dr}$$

where ρ is number density, dn is number of particles within the distance $r \rightarrow r + dr$ with respect to the chosen target particle. Given in figure 3 are the simulated $g_{Li^+-OC}(r)$ and $g_{Li^+-OW}(r)$ for the three systems. All $g_{Li^+-OC}(r)$ show peaks around r_{Li-OC} 2.2 Å for all systems. This peak position corresponds to the closest distance that Li^+ coordinates with OC in cluster. The $g_{Li^+-OW}(r)$ show peaks around r_{Li-OW} 2 Å for systems I and II. However, the peak for hydrated system I is much broader than half-hydrated system II. This result indicates that Li^+ tends to coordinate with water oxygen at 2 Å especially when half amount of water molecules were removed from the system. This observation may be explained as follows: in system I, the negatively charged OC atoms of the cluster and water oxygen atoms compete with each other to attract Li^+ and decrease the probability of Li^+ to coordinate with water oxygen. Therefore, the distribution peak at $r_{Li-OW} = 2$ Å is very broad. However, in system II, when half of the water molecules were removed, the remaining water molecules became more

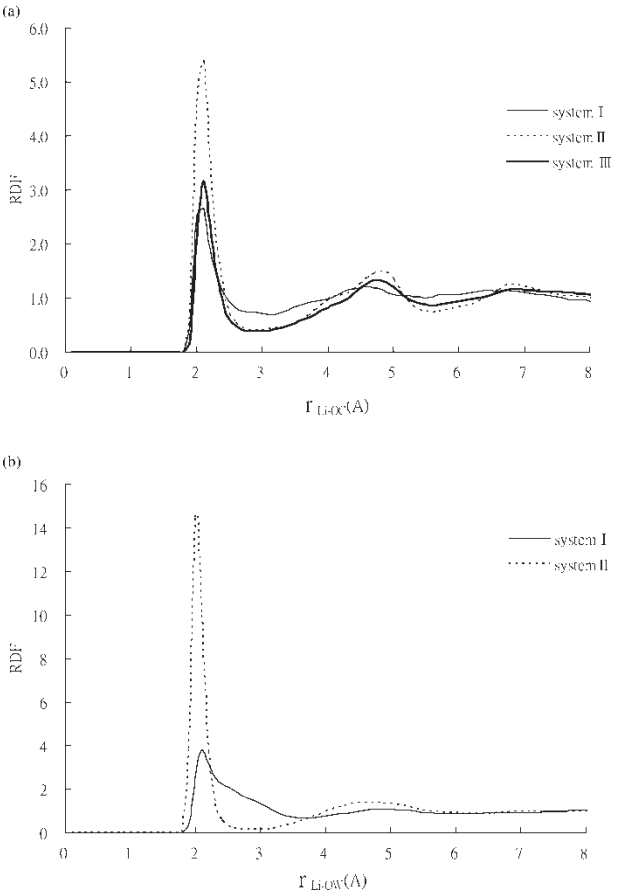

Figure 3. (a) RDF of Li^+ to OC of three simulated systems; (b) RDF of Li^+ to OW of simulated systems I and II.

mobile than in system I. This increases the probability of Li^+ to coordinate with water oxygen and results in a narrow distribution peak at $r_{Li-OW} = 2$ Å. In summary, we found that the mobility of Li^+ in POV system is larger than in that in a polymer matrix. This must be due to the large spacing between clusters, which allows Li^+ moves more easily in the system. On the other hand, the mobility of Li^+ increases as water molecules are eliminated from the system. This is because $[V_{10}O_{28}]^{6-}$ cluster contains many oxygen sites to attract positive ions; hence, decreases their selectivity to coordinate with the cluster.

Given in figure 4 are the calculated distances of a selected Li^+ to OC atoms on clusters in system III. The OC atoms and clusters are numbered for the convenience of analysis. The distance of Li^+ to OC is denoted as $d_{Li-O(n)}$, where n is the index of the OC atom. In the figure, OC atoms 33 and 1259 belong to the second cluster and 1105 OC atom belongs to the 18th cluster. The figure shows that originally the ion was in the neighborhood of OC atom 33 ($d_{Li-O(33)} = 2.2$ Å) and away from OC atoms 1259 and 1105 ($d_{Li-O(1259)} = 3.5$ Å, $d_{Li-O(1105)} = 5.0$ Å). After 1.0 ps, the ion moves to the neighborhood of the 1259th OC atom ($d_{Li-O(1259)} = 2.0$ Å) and away from the 33th OC atoms ($d_{Li-O(33)} = 2.7$ Å). At a 1.2 ps time the ion moves back to the neighborhood of the 33th OC ($d_{Li-O(33)} = 2.0$ Å) and away from form the 1259th OC ($d_{Li-O(1259)} = 3.3$ Å). At 15 ps, the ion suddenly moves to the

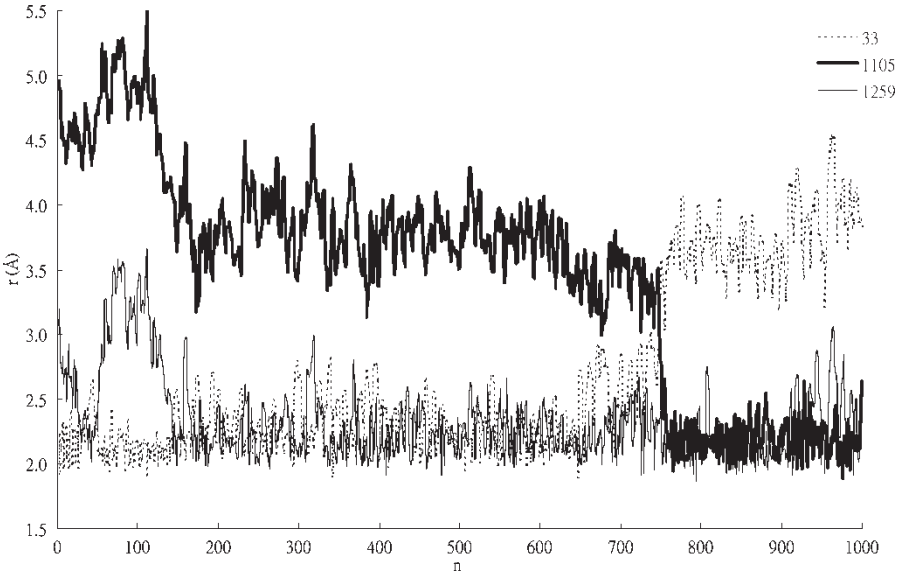

Figure 4. Distances of a Li^+ to selected OC atoms in completely dehydrated system III.

neighborhood of the 1105th OC atom ($d_{Li-O(1105)} = 2.0$ Å) and away from the 33th OC atom ($d_{Li-O(33)} > 3.0$ Å). These snapshots demonstrate that the lithium ion not only moved around OC atoms belonging to the same cluster, but also suddenly jumped from one cluster to another. The sudden jump can be regarded as a hopping motion between clusters. Given in figure 5 are the actual moving trajectories of lithium ions over the entire simulation period in completely dehydrated system III. In this figure only lithium ions with large displacements (more than 4.0 Å) were shown. The right side of this figure shows the trajectory of the selected lithium ion in an enlarged scale. The figure shows that the ion appears in three major regions as indicated. Regions I and II belong to the same cluster and region III belongs to another. The path from region II to III is clearly a hopping motion. After carefully analyzing our trajectories, we found that all lithium ions hop between clusters and the hopping frequency of Li^+ increases with decreasing of water molecules in the system. In all our simulated systems the magnitude of the Li^+ displacement is about 4–5 Å which is much larger than that in PEO system ($\sim$1.5 Å). The degree of freedom of Li^+ in the completely dehydrated system III is much larger than other two hydrated systems I and II.

In figure 5, we illustrate the calculated orientation correlation function, $C(t)$, of $[V_{10}O_{28}]^{6-}$ cluster in system III. The orientation of a cluster can be specified by three Euler angles (ϕ, θ, χ) between the molecular fixed system and space-fixed system. The normalized orientation

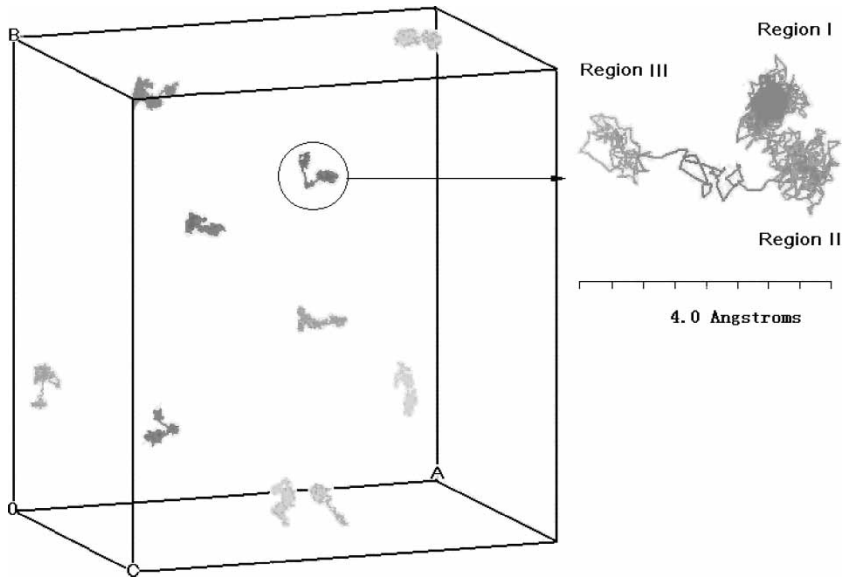

Figure 5. Trajectories of Li^+ ions in completely dehydrated system III.

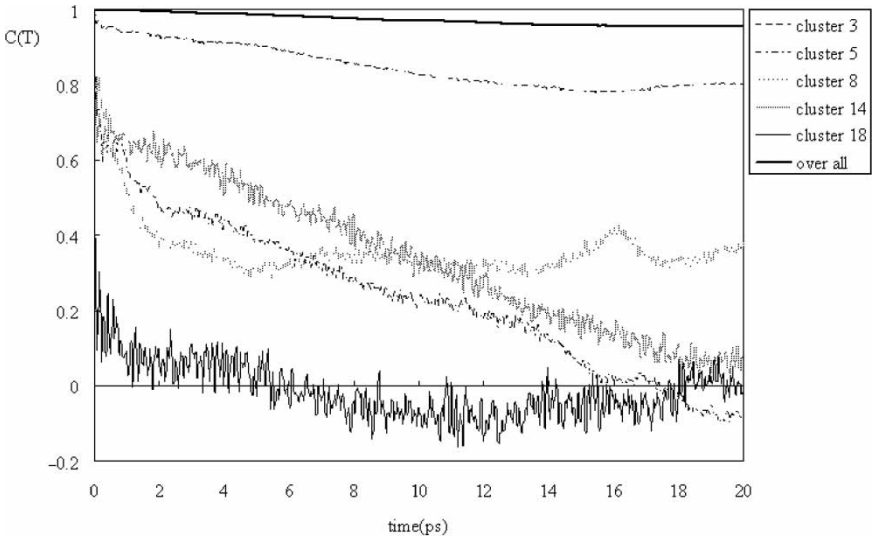

Figure 6. Orientation correlation functions of Euler angle θ of $[V_{10}O_{28}]^{-6}$ clusters in system III.

correlation function was calculated from the cosine of Euler angle θ,

$$C(t) = \frac{\langle \cos\theta(0)\cdot\cos\theta(t)\rangle}{\langle \cos\theta(0)\cdot\cos\theta(0)\rangle},$$

where the bracket indicates average over trajectory points. The figure shows the overall correlation function decays very slowly over the simulation time range, but some correlation functions of individual clusters decayed much rapidly. This indicates that these clusters rotate (tumble) much faster in the system. We believe that these rapidly rotating clusters result in large displacement of the lithium ion in the neighborhood of the clusters, substantiated by the drastic change of the distance of the lithium ion to the 1105 OC (18th cluster) shown in figure 4. From a different perspective, this behavior can be viewed as the hoping motion of the Lithium ion between clusters. For other two systems, we found similar behaviors of orientation correlation functions. Orientation correlation functions of some individual clusters decayed rapidly but overall correlation function decayed very slowly (figure 6).

Given in figure 7 are potential energy maps for a single lithium ion in the simulated cell of system III. To construct this map, the simulated cell was divided into $12 \times 12 \times 12$ grid points. A lithium ion was placed at each grid point and the interaction potential between this ion and other

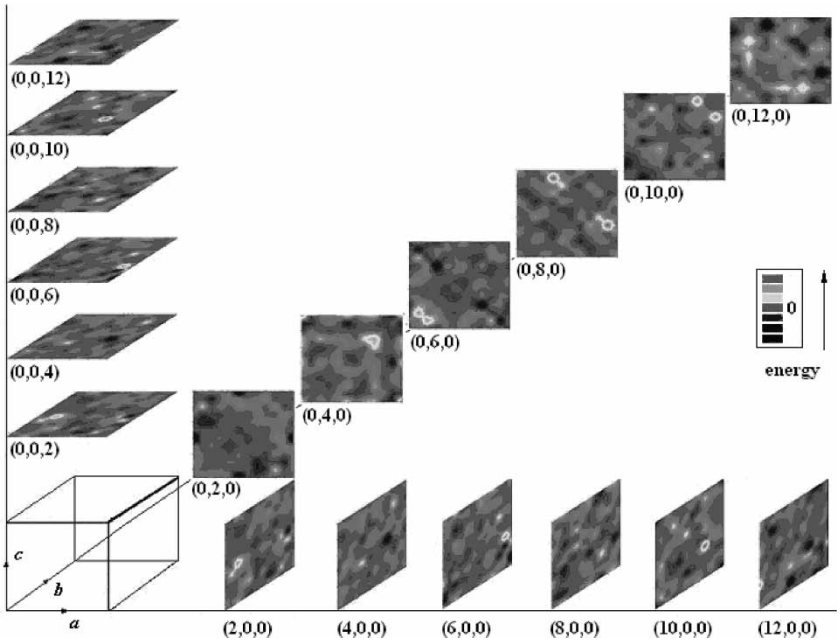

Figure 7. Interaction energy maps of a Li^+ in completely dehydrated system III.

charged ions and atoms of the cell was calculated by appropriate Ewald summation,

$$V_{\text{int}} = \sum_{i=1}^{N} \left(q_i q_{\text{Li}^+} \frac{\text{erfc}(\kappa|\vec{r}_{i-\text{Li}^+}|)}{|\vec{r}_{i-\text{Li}^+}|} + \frac{1}{\pi(abc)} \times \sum_{\vec{k}\neq 0} q_i q_{\text{Li}^+} \left(4\pi^2/k^2\right) \cos(\vec{k}\cdot\vec{r}_{i-\text{Li}^+}) \right)$$

where V_{int} is the interaction energy, q_{Li^+} is the charge (+1) of the lithium ion placed at grid point, $\vec{r}_{i-\text{Li}^+}$ is the vector from the ith charged atom to the ion, $\vec{k}$ is reciprocal wave vector, a,b,c are dimensions of the cell and erfc is the complementary error function, respectively. The parameter κ was set to $5/c$ and 200 wave vectors were used to obtain the interaction energy. The energy map was obtained by taking the average of the interaction potentials over all trajectory points at each grid point. In figure 7, we found that some low energy regions appeared along a, b and c directions in this system. This indicates that the motion of Li^+ is not restricted in any definite direction. In the half-hydrated system II, we found less low-energy regions than in system III, but more than in system I. The low-energy region is very limited in the fully hydrated system I. This indicates that the ion has a very restricted pathway inside system I. However, even in the fully hydrated system, the ion moves in all a, b and c directions. This indicates that isotropic moves of Li^+ in all POV systems.

4. Conclusion

This work investigates the migration of lithium ion in a very special material containing lithium ions, water and $[V_{10}O_{28}]^{6-}$ clusters. The simulation shows that the diffusive constant of lithium ion increases with the lowering of water content in the system. Although $[V_{10}O_{28}]^{6-}$ clusters are highly charged, our simulation shows that lithium ions do not stick to the cluster but can travel in the system with considerable mobility. The calculated conductivities due to the migration of lithium ions in these systems are much larger than typical values in the Li/polymer systems. Our theoretical simulation indicates that the lithium ions moved around the oxygen sites on the same cluster and also hopped between clusters. The major driving force for the hopping motion of lithium ion is due to: (1) rapid rotation of some individual $[V_{10}O_{28}]^{6-}$ clusters, (2) the highly negatively charged clusters, (3) many available oxygen sites in the cluster, and (4) large spacing between clusters in the system. These factors can rationalize the origin of the fast ion conduction of plastic crystal electrolytes. We also found that Li ion moved isotropically in all POV-contained systems. The density of amorphous dehydrated POAODH is at the same magnitude as the density of usual polymer systems. If this Li-$[V_{10}O_{28}]$ material can be doped into a polymer matrix (such as poly-ethylene oxide), then it may conduct lithium ion much better than Li/polymer systems. Although we do not have any experimental data to compare with the simulation results, however, we propose here that this Li-$[V_{10}O_{28}]^{6-}$ material can have large ionic conductivity. Future study on Li-$[V_{10}O_{28}]$ doped polymer system is underway.

References

[1] D. Handra, J.H. Helmes, A. Majumdar. Ionic conductivity in ordered and disordered phases of plastic crystals. *J. Electrochem. Soc.*, **141**, 1921 (1994).

[2] M. Hattori, S. Fukada, D. Nakamura, R. Ikeda. Studies of the anisotropic self-diffusion and reorientation of butyl ammonium cations in the rotator phases of butyl ammonium chloride using ^{1}H magnetic resonance, electrical conductivity and thermal measurements. *J. Chem. Soc. Faraday Trans.*, **86**, 3777 (1990).

[3] H. Ishida, Y. Furukawa, S. Kashino, S. Sato, R. Ikeda. Phase transitions and ionic motions in solid trimethylammonium iodide studied by ^{1}H and ^{127}I NMR, electrical conductivity, X-ray diffraction and thermal analysis. *Ber. Bunsenges. Phys. Chem.*, **100**, 433 (1996).

[4] T. Tanabe, D. Nakamura, R. Ikeda. Novel ionic plastic crystal phase of $[(CH_3)_4N]SCN$ obtainable above 455 K studied by proton magnetic resonance, electrical conductivity and thermal measurements. *J. Chem. Soc. Faraday Trans.*, **87**, 987 (1991).

[5] T. Shi,izu, S. Tanaka, N. Onoda-Yamamuro, S. Ishimaru, R. Ikeda. New rotator phase revealed in di-*n*-alkylammonium bromides studies by solid state NMR, powder XRD, electrical conductivity and thermal measurements. *J. Chem. Soc. Faraday Trans.*, **93**, 321 (1997).

[6] E.I. Cooper, C.A. Angell. Ambient temperature plastic crystal fast ion conductors (PLICFICS). *Solid State Ionics*, **18**, 570 (1986).

[7] R. Aronson, *et al.* Fast ion conductors with rotating sulphate ions. *J. Phys. Colloq. C6*, **41**, 35 (1980).

[8] R. Aronson, H.E.G. Knape, L.M. Torell. Brillouin spectra of the solid electrolyte Li_2SO_4. *J. Chem. Phys.*, **77**, 677 (1982).

[9] L. Borgesson, L.M. Torell. Reorientational motion in superionic sulphates: a Raman linewidth study. *Phys. Rev. B*, **32**, 2471 (1985).

[10] D.R. MacFarlane, J. Sun, M. Forysth, P. Meakin, N. Amini. Pyrrolidinium Imides: a new family of molten salts and conductive plastic crystal phases. *J. Phys. Chem.*, **103**, 4164 (1999).

[11] J. Sun, M. Forsyth, D.R. MacFarlane. Room temperature molten salts based on the quarternary ammonium ion. *J. Phys. Chem.*, **102**, 8858 (1998).

[12] D.B. Macfartane, J. Huang, M. Forsyth. Lithium-doped plastic crystal electrolytes exhibiting fast ion conduction for secondary batteries. *Nature*, **402**, 792 (1999).

[13] T.A. Skotheim, R.L. Elsenbaumer, J.R. Reynolds. *Handbook of Conducting Polymers*, Marcel Dekker, New York (1998).

[14] F.M. Gray. *Solid Polymer Electrolytes*, VCH Publisher, Inc, New York (1991).

[15] Y. Okamoto, Z.S. Xu, M.G. McLin, J.J. Fontanella, Y.S. Pak, S.G. Greenbaum. Synthesis and properties of a cation-conducting, high temperature polymer electrolyte. *Solid State Ionics*, **60**, 131 (1993).

[16] S. Kim, D.A. Cameron, Y. Lee, J.R. Reynolds, C.S. Savage. Aromatic and rigid rod polyelectrolytes based on sulfonated poly(benzobisthiazoles). *J. Polym. Sci.; Polym. Chem. Ed.*, **A34**, 481 (1996).

[17] J.T. Wang, J.S. Wainright, R.F. Savinell, M. Litt. A direct methanol fuel cell using acid-doped polybenzimidazole as polymer electrolyte. *J. Appl. Electrochem.*, **26**, 751 (1996).

[18] P.T. Boinske, L.A. Curtiss, J.W. Halley, B. Lin, A. Sutjianto. Lithium ion transport in a model of amorphous polyethylene oxide. *J. Computer-Added Mater. Design*, **3**, 385 (1996).

[19] A. Sutjianto, L.A. Curtiss. Theoretical study of the potential energy surface of diglyme. *Chem. Phys. Lett.*, **264**, 127 (1997).

[20] T. Arimura, D. Ostrovskii, T. Okada, G. Xie. The effect of additives on the ionic conductivity performances of perfluoroalkyl sulfonated ionomer membranes. *Solid State Ionics*, **118**, 1 (1999).

[21] F. Müller-Plathe, W.F. van Gunsteren. Computer simulation of a polymer electrolyte: lithium iodide in amorphous poly(ethylene oxide). *J. Chem. Phys.*, **103**, 4745 (1995).

[22] P. Johansson. First principles modeling of amorphous polymer electrolytes: Li^+–PEO, Li^+–PEI, and Li^+–PES complexes. *Polymer*, **42**, 4367 (2001).
[23] S. Neyertz, D. Brown, J. Thomas. Molecular dynamics simulation of crystalline poly(ethylene oxide). *J. Chem. Phys.*, **101**, 10064 (1994).
[24] S. Neyertz, D. Brown. A computer simulation study of the chain configurations in poly(ethylene oxide)-homolog melts. *J. Chem. Phys.*, **102**, 9725 (1995).
[25] J.W. Halley, Y. Duan, L.A. Curtiss, A.G. Baboul. Lithium perchlorate ion pairing in a model of amorphous polyethylene oxide. *J. Chem. Phys.*, **111**, 3302 (1999).
[26] J.A. Johnson, M.-L. Saboungi, D.L. Price, S. Ansell, T.P. Russell, J.W. Halley, B. Nielsen. Atomic structure of solid and liquid polyethylene oxide. *J. Chem. Phys.*, **109**, 7005 (1998).
[27] O. Borodin, G.D. Smith. Molecular dynamics simulations of poly(ethylene oxide)/LiI melts. 2. Dynamic properties. *Macromolecules*, **33**, 2273 (2000).
[28] J.W. Halley, Y. Duan, B. Nielsen, P.C. Redfern, L.A. Curtiss. Simulation of polyethylene oxide: improved structure using better models for hydrogen and flexible walls. *J. Chem. Phys.*, **115**, 3957 (2001).
[29] Y. Duan, J.W. Halley, L. Curtiss, P. Redfern. Mechanisms of lithium transport in amorphous polyethylene oxide. *J. Chem. Phys.*, **122**, 054702 (2005).
[30] A.L. Xie, C.A. Ma. Hexalithium hexadecahydrate decavanadate, $[Li_6(H_2O)_{16}V_{10}O_{28}]_n$. *Acta Cryst. C*, **C61**, i67 (2005).
[31] D. Becke. Density-functional exchange-energy approximation with correct asymptotic behavior. *Phys. Rev. A*, **38**, 3098 (1988).
[32] C. Lee, W. Yang, R.G. Parr. Development of the Colle-Salvetti correlation-energy formula into a functional of the electron density. *Phys. Rev. B*, **37**, 785 (1988).
[33] J.P. Perdew. Density-functional approximation for the correlation energy of the inhomogeneous electron gas. *Phys. Rev. B*, **33**, 8822 (1986).
[34] M.C. Zerner, G.H. Loew, R.F. Kirchner, U.T. Mueller-Westerhoff. An intermediate neglect of differential overlap technique for spectroscopy of transition-metal complexes. Ferrocene. *J. Am. Chem. Soc.*, **102**, 589 (1980).
[35] W.L. Jorgensen. Quantum and statistical mechanical studies of liquids. 10. Transferable intermolecular potential functions for water, alcohols, and ethers. Application to liquid water. *J. Am. Chem. Soc.*, **103**, 335 (1981).
[36] S.L. Mayo, B.D. Olafson, W.A. Goddard. DREIDING: a generic force field for molecular simulations. *J. Phys. Chem.*, **94**, 8897 (1990).
[37] L.V. Woodcock, K. Singer. Thermodynamic and structural properties of liquid ionic salts obtained by Monte Carlo computation. Part 1.—Potassium chloride. *Trans. Faraday Soc.*, **67**, 12 (1971).
[38] Accelrys Inc. Cerius2 user guide 4.5 (2000).